npg

The plasma membrane channel ORAI1 mediates detrimental calcium influx caused by endogenous oxidative stress

N Henke[1], P Albrecht[1], I Bouchachia[1], M Ryazantseva[2], K Knoll[1], J Lewerenz[3], E Kaznacheyeva[2], P Maher[4] and A Methner*,[1,5]

The mouse hippocampal cell line HT22 is an excellent model for studying the consequences of endogenous oxidative stress. Addition of extracellular glutamate depletes the cells of glutathione (GSH) by blocking the glutamate − cystine antiporter system x_c^-. GSH is the main antioxidant in neurons and its depletion induces a well-defined program of cell death called oxytosis, which is probably synonymous with the iron-dependent form of non-apoptotic cell death termed ferroptosis. Oxytosis is characterized by an increase of reactive oxygen species and a strong calcium influx preceding cell death. We found a significant reduction in store-operated calcium entry (SOCE) in glutamate-resistant HT22 cells caused by downregulation of the Ca^{2+} channel ORAI1, but not the Ca^{2+} sensors STIM1 or STIM2. Pharmacological inhibition of SOCE mimicked this protection similarly to knockdown of ORAI1 by small interfering RNAs. Long-term calcium live-cell imaging after induction of the cell death program showed a specific reduction in Ca^{2+}-positive cells by ORAI1 knockdown. These results suggest that dysregulated Ca^{2+} entry through ORAI1 mediates the detrimental Ca^{2+} entry in programmed cell death induced by GSH depletion. As this detrimental Ca^{2+} influx occurs late in the course of the cell death program, it might be amenable to therapeutic intervention in diseases caused by oxidative stress.

Oxidative stress is a phenomenon involved in a broad range of pathological conditions of the nervous system such as Alzheimer's and Parkinson's disease, stroke and trauma. It is provoked by an imbalance between superoxide production in the mitochondria and insufficient clearance of reactive oxygen species (ROS) through antioxidative defense mechanisms of the cell. One major defense pathway of nerve cells against ROS depends on the production of glutathione (GSH), a tripeptide composed of glutamate, cysteine and glycine, via the enzymes glutamate − cysteine ligase and GSH synthetase. In its reduced state, GSH serves as electron donor to detoxify ROS and is thereby oxidized to form GSH disulfide. The recovery of GSH from GSH disulfide is mediated by GSH reductase under NADPH consumption.[1]

GSH depletion serves to study the effects of endogenous oxidative stress and can be excellently studied in vitro by treating cells with glutamate, which inhibits cystine uptake through the glutamate/cystine antiporter system x_c^-. Within the cell, cystine is rapidly converted to cysteine, the rate-limiting amino acid for GSH synthesis. Cystine deprivation then causes secondary GSH depletion and a programmed cell death by oxytosis or oxidative glutamate toxicity, which is clearly distinct from apoptosis, necrosis, and cell death associated with autophagy, but probably synonymous with the recently described iron-dependent form of non-apoptotic cell death termed ferroptosis, which seems to be involved in the selective elimination of some tumor cells and protection from neurodegeneration.[2]

A well-established model system for oxytosis/ferroptosis is glutamate-induced cell death in the hippocampal cell line HT22, which has been used extensively to clarify the cascade leading to cell death and to identify antioxidant pathways and

[1]Department of Neurology, Heinrich-Heine Universität Düsseldorf, Düsseldorf, Germany; [2]Institute of Cytology St. Petersburg, St. Petersburg, Russia; [3]University of Ulm, Department of Neurology, Ulm, Germany; [4]Cellular Neurobiology Laboratory, Salk Institute for Biological Studies, La Jolla, CA, USA and [5]Focus Program Translational Neuroscience (FTN), Rhine Main Neuroscience Network (rmn²), Johannes Gutenberg University Medical Center Mainz, Department of Neurology, Mainz, Germany
*Corresponding author: Professor A Methner, Focus Program Translational Neuroscience (FTN), Rhine Main Neuroscience Network (rmn²), Johannes Gutenberg University Medical Center Mainz, Department of Neurology, Langenbeckstr. 1, D-55131 Mainz, Germany, Tel: + 49 6131 17 2695, Fax: + 49 6131 17 5967; Email: axel.methner@gmail.com

proteins (reviewed in[3]). In this system, GSH depletion leads to an exponential increase in ROS that mostly originates from mitochondrial complex I activity.[4] After ~6 h of glutamate exposure, the lipid-oxidizing enzyme 12/15-lipoxygenase (12/15- LOX; EC 1.13.11.33) is activated and generates 12- and 15- hydroxyeicosatetraenoic acids[5] that directly damage mitochondria, and cause mitochondrial depolarization and increased ROS production.[6] The eicosanoids produced by 12-LOX are, however, also activators of soluble guanylate cyclases and thereby increase the concentration of intracellular cyclic guanosine monophosphate (cGMP), resulting in a detrimental influx of calcium at the end of the cell death cascade through a yet uncharacterized cGMP-dependent calcium channel.[7] This Ca^{2+} influx is essential for the completion of the cell death program, as proven by the fact that glutamate-treated HT22 cells do not die when Ca^{2+} influx is blocked by $CoCl_2$ or in Ca^{2+}-free medium,[7–9] but the molecular identity of the contributing Ca^{2+} channels is still unknown.

To identify the mechanism of Ca^{2+} entry in the final phase of oxidative glutamate toxicity, we compared the cellular calcium state of glutamate-sensitive and resistant HT22 cells, which are resistant due to the increased expression of various proteins with antioxidant properties,[10–13] and found an isolated attenuation of store-operated calcium entry (SOCE) in the resistant cells. SOCE is activated when the endoplasmic reticulum (ER), the main cellular calcium store, is depleted, for example,. during inositol trisphosphate (IP3)-mediated signaling events. When a membrane receptor is activated by its ligand, IP3 is generated near the plasma membrane and quickly diffuses through the cytoplasm to reach its receptor (Inositol trisphosphate receptor, IP3R) at the ER membrane. Binding of IP3 to IP3R releases Ca^{2+} stored in the ER lumen and generates a cytosolic Ca^{2+} signal, resulting in ER Ca^{2+}-store depletion. To refill the ER, plasma membrane Ca^{2+} channels need to be activated to permit Ca^{2+} entry from the extracellular space, so-called SOCE. The molecule that transmits the information of $[Ca^{2+}]_{ER}$ to plasma membrane Ca^{2+} channels is stromal interaction molecule 1 (STIM1).[14,15] STIM1 clusters into punctae close to the plasma membrane upon store depletion and binds and activates ORAI1, a plasma membrane calcium channel.[16–18]

In this study, we provide evidence that dysregulated SOCE through ORAI1 is the main calcium entry mechanism during oxidative glutamate toxicity, suggesting that SOCE inhibition might be a valuable tool in the treatment of diseases associated with increased oxidative stress.

Results

Reduced store-operated Ca^{2+} entry in hippocampal cells resistant to oxidative stress. Glutamate-resistant HT22 cells are protected against oxidative glutamate toxicity (Figure 1a) mainly via an elevated GSH content due to an increased expression of the glutamate/cystine antiporter subunit xCT.[19] They also show an increased expression of other proteins with antioxidant properties.[10,11,13] We therefore reasoned that the function and expression of the sought-after detrimental Ca^{2+} channel might be altered in these cells and studied the content of the main cellular

Ca^{2+} store, the ER, by staining the cells with the ratiometric Ca^{2+}-sensitive dye Fura2 followed by treatment with the irreversible sarcoplasmic/ER Ca^{2+}-ATPase (SERCA) inhibitor thapsigargin, which resulted in the expected biphasic cytosolic Ca^{2+} rise. Although HT22S and R cells behaved similarly during the first phase of Ca^{2+} rise, which corresponds to Ca^{2+} passively leaking out of the ER, the second phase of cytosolic Ca^{2+} rise was remarkably reduced in HT22R compared with HT22S cells (Figure 1b).
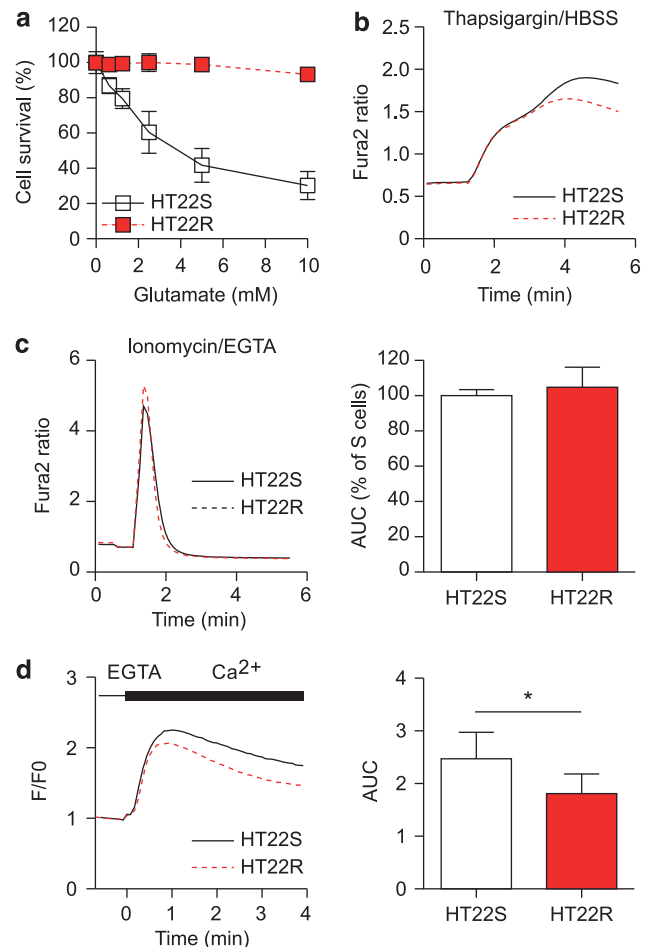

Figure 1 Reduced store-operated Ca^{2+} in hippocampal cells resistant to oxidative stress. (**a**) 5000 glutamate-sensitive and -resistant HT22S and R cells were seeded into 96-well plates and subjected to the indicated concentrations of glutamate 24 h later; viability was quantitated again 16 h later with the cell-titer blue reagent. Mean ± S.E.M. fluorescence values of three replicates obtained in three independent experiments were plotted against the glutamate concentration. (**b − d**) Fura2-live-cell imaging of glutamate-sensitive and -resistant HT22S and R cells. (**b**) After 1 min of baseline recording in HBSS, 2 μM of thapsigargin was added and the fura2 signal recorded for an additional 4 min. (**c**) After 30 s of baseline recording in HBSS with Ca^{2+}, EGTA was added. After a further 30 s, 5 μM of ionomycin was applied and the fura2 signal recorded for the following 4 min. (**d**) For measurement of SOCE, ER Ca^{2+} stores of HT22S and R cells were depleted by incubation in EGTA buffer supplemented with 2 μM thapsigargin. After 6 min of store depletion, the buffer was exchanged with HBSS supplemented with 1.26 mM Ca^{2+} and SOCE was recorded. Graph shows only Ca^{2+} readdition after store depletion. Graphs 1b and c show mean fura2 ratio of 20 − 30 individually-measured wells for each condition, containing altogether 2000 − 3000 cells. Graph 1d is pooled from nine wells for each condition containing > 260 cells. For C and D, the area under the curve was calculated and plotted as mean ± S.E.M. in bar graphs. *$P < 0.05$
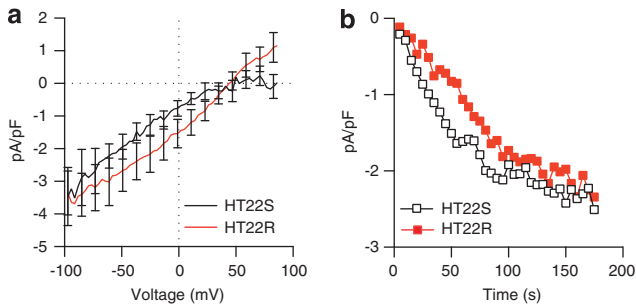
Figure 2 Different SOCE current characteristics in HT22S and glutamate-resistant HT22R cells. (**a**) Average I/V relationships for currents evoked by passive depletion of Ca^{2+} stores with 1 μM thapsigargin in HT22S (*black, n* = 6) and HT22R (*red, n* = 11) cells. The I/V relationships were measured when the currents reached the maximum. The data are shown as mean ± S.E.M., $P < 0.05$. (**b**) The average amplitude of SOCE currents recorded in whole-cell experiments is shown as a function of time after application of 1 μM thapsigargin to HT22S (black, n = 6) and HT22R (red, n = 11) cells. The current amplitudes were measured at each ramp at –80 mV test potentials. The data are shown as mean

We hypothesized that this second plateau corresponds to reduced SOCE and decided to delve further into this.

To distinguish between Ca^{2+} leaking from the ER and Ca^{2+} entering from outside the cell, we measured the whole-cellular Ca^{2+} store content and SOCE separately. Fura2-based Ca^{2+} live-cell imaging yielded no significant difference between HT22S and HT22R in the cytosolic Ca^{2+} rise induced by treatment with the Ca^{2+} ionophore ionomycin, which releases the whole-cellular Ca^{2+} content from the intracellular stores (Figure 1c). For measurement of SOCE activity, we depleted the ER Ca^{2+} store by addition of thapsigargin in EGTA buffer. After 6 min of store depletion, Ca^{2+} was readded and Ca^{2+} influx corresponding to SOCE was measured. In line with the data shown in Figure 1b, SOCE activity was significantly reduced in HT22R cells (Figure 1d).

To verify the reduced SOCE capacity of HT22R cells at the single cell level, we assessed SOCE activity by electrophysiological recordings using the whole-cell patch-clamp technique. Currents were evoked by application of 1 μM thapsigargin to achieve ER store depletion. Consistent with our results obtained in fura2 life − cell imaging experiments, HT22S and HT22R cells demonstrated different SOCE current − voltage (I/V) relation (Figure 2a). SOCE currents in HT22S cells revealed an inward rectification as expected for I_{CRAC} currents provided by ORAI1 channels, whereas SOCE currents in HT22R cells demonstrated a linear I/V relation with a reversal potential around + 40 mV. There was no difference in amplitude or speed of SOCE currents development in time in HT22S and HT22R cells (Figure 2b). These data are in line with an altered composition or abundance of I_{CRAC} channels in HT22R cells. We therefore set out to investigate the role of SOCE during oxidative glutamate toxicity.

Prolonged oxidative stress reduces the ER Ca^{2+} content and SOCE activity. Glutamate-resistant HT22R cells were continuously cultivated in medium containing 10 mM glutamate to preserve their resistant phenotype. To test whether glutamate directly or indirectly influences SOCE capacity, we aimed to measure SOCE activity in glutamate-treated HT22S cell. We also hypothesized that cytosolic cGMP might

influence the SOCE capacity similarly to glutamate because the Ca^{2+} influx leading to cell death by oxytosis is preceded by a cytosolic increase of cGMP.[7] Application of 8-(4-chlorophenylthio)-guanosine 3′,5′-cyclic monophosphate (pCPT-cGMP), a cell-permeable cGMP analog, indeed induced death of HT22 cells in a concentration-dependent manner (Figure 3a) and opened plasma membrane Ca^{2+} channels resulting in a slow but pronounced cytosolic Ca^{2+} rise, which we measured with the genetically-encoded Ca^{2+} sensor GCaMP5, expressed from a bicistronic transcript together with the red fluorescent protein (RFP), to normalize the GCaMP5 signal to the level of transfection (Figure 3b).

We elicited SOCE by store depletion through thapsigargin-induced SERCA inhibition under Ca^{2+}-free conditions and subsequent restitution of Ca^{2+}. After 8 h of incubation with either glutamate or pCPT-cGMP, HT22S cells showed a reduced $[Ca^{2+}]_{ER}$ and reduced SOCE (Figure 3c). Addition of pCPT-cGMP or glutamate directly at the onset of measurement had no effect (Figure 3d). We therefore hypothesized that this reduction in $[Ca^{2+}]_{ER}$ and SOCE after induction of the cell death program might be a consequence of the endogenous oxidative stress that eventually kills the cells. And indeed, preventing oxidative stress with the antioxidant N-acetyl-L-cysteine (NAC) protected glutamate-treated cells from cell death (Figure 3e), and partially rescued the ER Ca^{2+} content as well as the SOCE capacity after 8 h of treatment (Figure 3f).

These results were of course not in line with our hypothesis that increased SOCE mediates the cytotoxic Ca^{2+} influx at the end of the cascade leading to cell death. We reasoned that the cell death program, which is already irreversible after 8 h of glutamate or 8-pCPT-cGMP treatments, alters many aspects of the intracellular Ca^{2+} homeostasis, which might obscure the effects on SOCE. We therefore decided to study the effect of SOCE on glutamate- and cGMP-induced cell death pharmacologically.

Pharmacological inhibition of SOCE protects against oxidative stress. We treated HT22 cells with a pharmacological inhibitor of SOCE, 2-aminoethoxydiphenyl borate (2-APB), and induced oxidative stress by addition of glutamate. 2-APB concentration-dependently protected against glutamate toxicity (Figure 4a) even when added up to 8 h after glutamate addition (Figure 4b). We also tested the ability of 2-APB to protect from pCPT-cGMP-induced cell death and observed a remarkable protective effect of 2-APB under these conditions, which was even stronger than that of the general Ca^{2+}-channel blocker $CoCl_2$ (Figure 4c). As 2-APB is a well-known inhibitor of SOCE and protects HT22 cells from oxidative glutamate toxicity and pCPT-cGMP even when applied several hours after induction of oxidative stress, these observations support the hypothesis that the detrimental, late-onset Ca^{2+} influx induced by endogenous oxidative stress is mediated via components of the SOCE machinery.

The SOCE Ca^{2+} influx channel ORAI1 is downregulated in glutamate-resistant HT22R cells. After clarifying that the observed reduction of SOCE in HT22R cells (Figures 1d
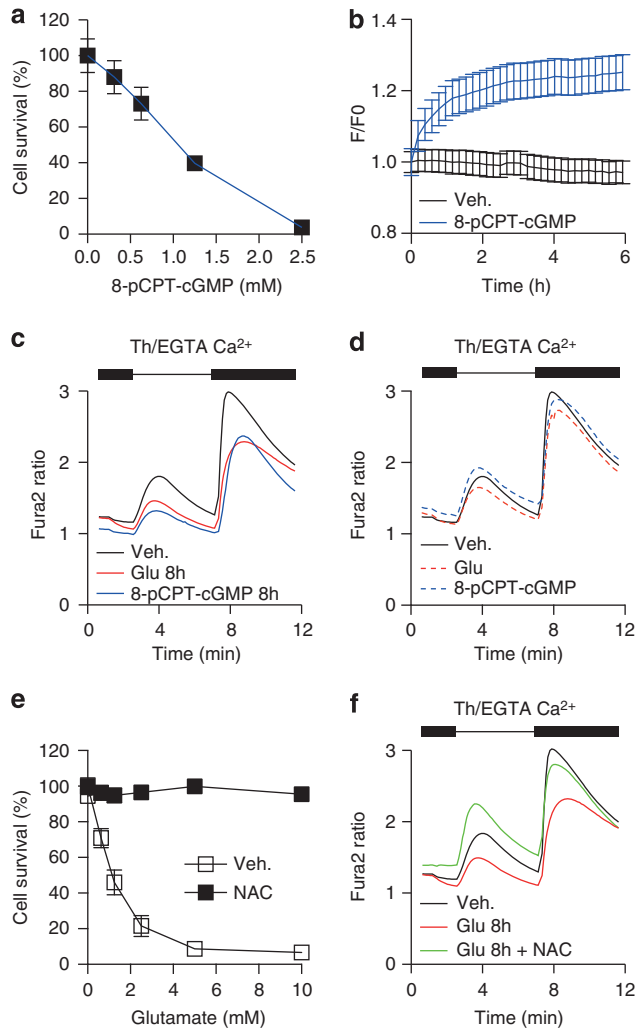
Figure 3 Prolonged oxidative stress reduces the ER Ca^{2+} content and SOCE activity. (**a**) Application of pCPT-cGMP-induces cell death in HT22 cells. Cells were subjected to the indicated concentrations of pCPT-cGMP and viability was measured 16 h later with the cell-titer blue reagent. The graph shows the mean fluorescence values ± S.E.M. of 11 replicate wells measured in two independent experiments plotted against glutamate concentration. (**b**) GCaMP5-based long-term Ca^{2+} live-cell imaging experiments reveals a pCPT-cGMP-induced cytosolic Ca^{2+} increase. Graphs show mean normalized GCaMP/RFP ratio of 10 wells each containing > 30 cells obtained in two independent experiments. (**c**, **d** and **f**) Fura2-based SOCE measurements performed on a BD Pathway high content imaging system. Cells were either preincubated for 8 h with 2.5 mM glutamate, 2.5 mM glutamate together with 2 mM NAC or 2.5 mM pCPT-cGMP or supplemented with these substances directly at the onset of measurement as indicated. For measurement of SOCE after baseline recording in HBSS, ER Ca^{2+} stores were depleted by addition of 2 μM thapsigargin in 2 mM EGTA, which was necessary to bind the Ca^{2+} ions of the HBSS buffer. After 6 min of store depletion, 5 mM of Ca^{2+} was added to overload the EGTA and allow SOCE. Ca^{2+} influx was recorded for additional 4 min. Each trace represents the mean of five to six wells measured in three independent experiments. (**e**) Oxidative stress was induced in NAC or vehicle treated cells by application of indicated amounts of glutamate. Cell viability was quantitated 16 h after oxidative stress onset with the cell-titer blue reagent. The graph shows the mean ± S.E.M. of nine replicate wells measured in three independent experiments plotted against glutamate concentration

Figure 4 Pharmacological inhibition of SOCE protects against oxidative stress. (**a**) 2-APB or vehicle treated HT22S cells were subjected to oxidative stress by addition of the indicated amounts of glutamate. 16 h after stress onset, viability was quantitated with the CTB assay and normalized to controls without glutamate. Graphs show mean ± S.E.M. of nine replicates obtained in three independent experiments. (a right panel) The indicated concentrations of 2-APB were added to HT22 cells treated with 5 mM of glutamate. 20 h after stress, onset viability was quantified with the MTT-viability assay. (**b**) 2-APB was added to glutamate (5 mM)-treated HT22 cells at the indicated times after glutamate addition. After 20 h, cell viability was quantified by the MTT-assay. (**c**) Cells were treated with the indicated concentrations of 2-APB, CoCl$_2$ or vehicle and the MTT-assay was performed 20 h after addition of 2.5 mM pCPT-cGMP

and 2a) is relevant for the resistance against oxidative stress, we decided to identify the involved proteins. Resistance against oxidative stress in HT22R cells is mediated in part via
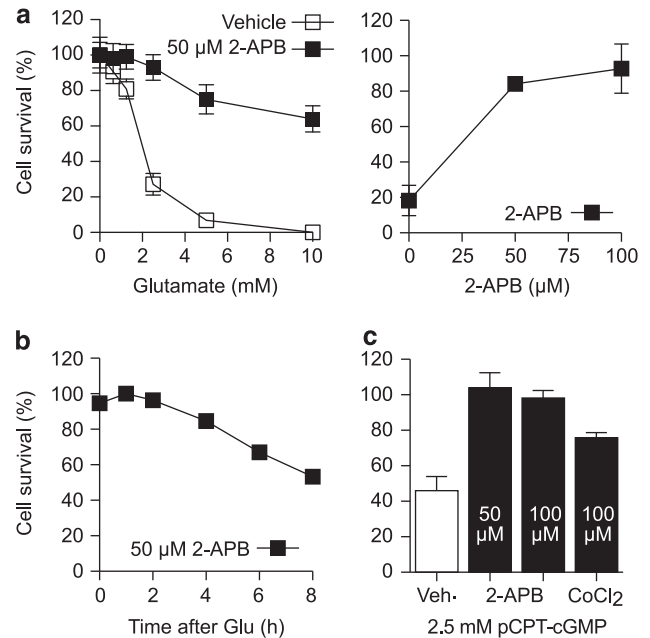
transcriptional regulation of protective proteins.[10,11,13] We therefore hypothesized that the reduced SOCE observed in HT22R cells might be mediated via downregulation of components of the cellular SOCE machinery and analyzed the expression pattern of the SOCE-contributing proteins STIM1, STIM2 and ORAI1, as well the transient receptor potential melastatin 7 (TRPM7) channel, a Ca^{2+} permeable channel that is also blocked by 2-APB.[20] The protein levels of STIM1 and STIM2 were equal in HT22S and R (Figure 5a and b). TRPM7 expression was analyzed by quantitative real-time-PCR (qRT-PCR) and also found to be the similar in both cell types (Figure 5c). Immunoblotting against ORAI1 produced a ladder of bands between 50 and 100 kDa, which may be due to protein modifications for example, glycosylation, differential splicing,[21] dimerization or even tetramerization.[22] We quantified the 50 kDa band, which according to the datasheet of the antibody, should be ORAI1 and the more prominent 80 kDa band. Both bands were significantly downregulated in HT22R cells (Figure 5d), consistent with the reduced SOCE activity in these cells. Downregulation of these bands by small inhibitory RNA (siRNA) transfection, which correlated with mRNA quantification by RT-PCR (Figure 6h and i), also suggested specificity of the antibody used.

These results pointed to ORAI1 as being the protein that mediates the reduced SOCE observed in HT22R cells. To
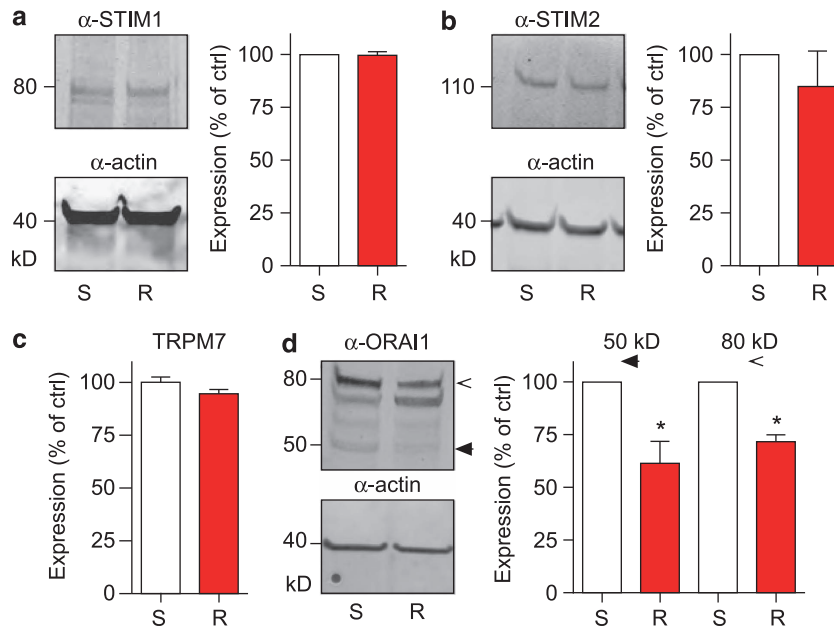
Figure 5 The SOCE Ca^{2+} influx channel ORAI1 is downregulated in glutamate-resistant HT22R cells. Expression analysis of key SOCE players and TRPM7 in HT22S and R cells. (**a, b** and **d**) Immunoblots were probed with antibodies against STIM1 (**a**) or 2 (**b**) and ORAI1 (**d**); GAPDH served as loading control and was simultaneously recorded with the protein of interest on the same membrane with the Licor infrared imaging system. Quantification of immunoblots was done with ImageJ software. Intensity values were normalized to HT22S samples and plotted in bar graphs as expression in percentage. (**c**) RT-PCR analysis of *TRPM7* expression level in HT22S and R cells. The *TRPM7* signal was normalized to the endogenous control *hprt* and plotted as mean expression level ± S.E.M. in percentage. All graphs show the mean of at least three independently performed experiments. *$P < 0.05$ using students *t*-test

complement this and to show that this downregulation is indeed involved in the resistance against oxidative stress observed in HT22R cells, we decided to knockdown the components of the SOCE machinery, STIM1, STIM2, ORAI1 and TRPM7 by siRNA and determine the susceptibility of the cells to oxidative glutamate toxicity.

Knockdown of ORAI1 protects from GSH depletion. We transfected HT22 cells with two different siRNAs against STIM1, STIM2 ORAI1 or TRPM7 and treated these cells with glutamate or L-buthionine-(S,R) sulfoximine (BSO), an inhibitor of the rate-limiting enzyme glutamate-cysteine ligase, 48 h after transfection. Successful knockdown was verified by RT-PCR analysis (Figure 6a, d, f and h) and immunoblotting (Figure 6b and i). In line with the protein expression pattern observed in glutamate-resistant cells (Figure 5), knockdown of STIM1 or STIM2 induced no significant protective effect against GSH depletion elicited either by glutamate or BSO (Figure 6c and e), whereas reduced ORAI1 levels strongly protected HT22 cells from oxidative stress (Figure 6j). Interestingly, siRNA-mediated knockdown of TRPM7 in HT22S cells significantly increased susceptibility to oxidative glutamate toxicity (Figure 6g).

We conclude from these data that the protective effect of 2-APB is unlikely to involve STIM1, STIM2 or TRPM7 inhibition, as reduction of these Ca^{2+} entry modulating proteins has either no or even the opposite effect of 2-APB. Rather, two lines of evidence suggest that ORAI1 is involved in oxidative stress-induced Ca^{2+} influx: ORAI1 is downregulated in glutamate-resistant cells and its knockdown protects

glutamate-sensitive cells from cell death mediated by GSH depletion. We conclude that the protective effect of 2-APB is mediated by the inhibition of ORAI1-mediated Ca^{2+} influx and that reduced expression of ORAI1 is involved in the resistance of HT22R cells against oxidative stress.

Knockdown of ORAI1 inhibits cytosolic calcium elevation during oxytosis. To directly investigate the contribution of ORAI1 to the detrimental Ca^{2+} influx induced by glutamate, we continued with long-term Ca^{2+} live-cell imaging experiments to visualize the cytosolic Ca^{2+} rise during oxytosis. We transfected HT22 cells with the two different siRNAs against ORAI1 (Figure 6h, i) or non-targeting control-siRNA together with the Ca^{2+}-sensor GCaMP5. Knockdown efficiency was controlled by RT-PCR (data not shown). 48 h after transfection, the cells were exposed to glutamate overnight and the cytosolic calcium signal was monitored in a high-content microscope equipped with an environmental chamber to keep the temperature and CO_2 concentration constant. Two hours after glutamate addition, we started to acquire the GCaMP and the control RFP signal every 15 min for the next 14 h and calculated the GCaMP/RFP ratio. This showed that cells peak in a seemingly random manner between 5 – 16 h of glutamate exposure. After a sharp increase in GCaMP signal, the cells quickly lyse, which was visible through vigorous quenching of GCAMP and RFP fluorescence. A typical sequence of pictures is shown in Figure 7a. The appearance of these Ca^{2+} spikes was highly asynchronously spread over the whole-time frame (Figure 7a lower panel) and significantly less frequent in ORAI1 – siRNA-transfected cells compared
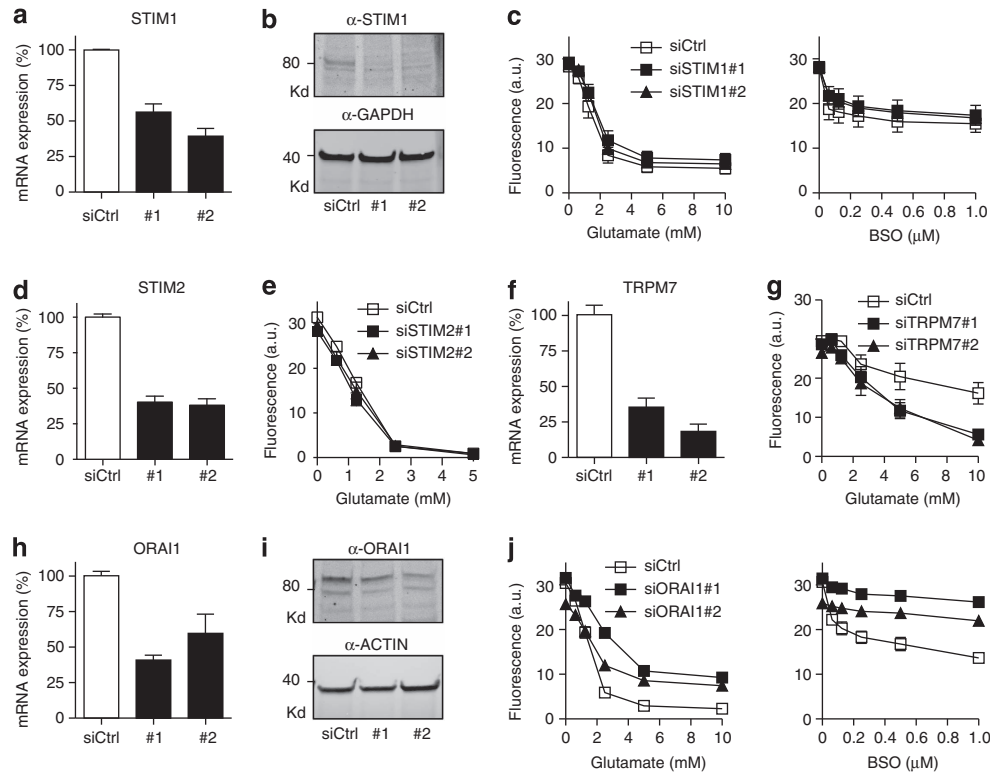
Figure 6 Knockdown of ORAI1 protects from GSH depletion. HT22S cells were transfected with two independent siRNAs against *STIM1, STIM2, ORAI1* and *TRPM7* or with non-targeting control siRNA and 48 h later subjected to cell survival experiments. **(a, d, f** and **h)** RT-PCR analyses of successful knockdown of *STIM1* **(a)**, *STIM2* **(d)**, *ORAI1* **(h)** and *TRPM7* **(f)**. Signals of genes of interest were normalized to *hprt* and plotted as expression in percentage relative to control-siRNA transfected samples. **(b** and **i)** Verification of successful knockdown by immunoblot. The membranes were simultaneously probed with antibody against either STIM1 **(b)** or ORAI1 **(i)** and GAPDH respectively actin as loading control and analyzed with the Licor infrared imaging system. **(c, e, g** and **j)** Survival experiments of siRNA-transfected cells. The indicated amounts of glutamate or BSO were added 48 h after transfection and viability was quantified with the CTB reagent 16 h after glutamate or BSO addition. The graphs show the mean fluorescence ± S.E.M. of 15 replicates obtained in three independent experiments plotted against glutamate or BSO concentration

with scrambled siRNA-transfected cells (Figure 7b). We also treated ORAI1 siRNA-transfected cells with pCPT-cGMP and immediately recorded the cytosolic Ca^{2+} level with GCaMP5 as described above. Interestingly, pCPT-cGMP did not evoke Ca^{2+} peaks similar to glutamate, but instead induced a slow but prominent cytosolic Ca^{2+} influx (Figure 3b). Because the cytosolic Ca^{2+} increase induced by cell-permeable cGMP occurs with a steady increase, we calculated the slope of Ca^{2+} influx over the first 2 h, which was significantly reduced by downregulation of ORAI1 (Figure 7c).

We conclude from these results that the SOCE-mediating channel protein ORAI1 significantly contributes to the detrimental Ca^{2+} influx elicited by cGMP or caused by oxidative stress in the course of GSH depletion.

Discussion

We conclude that ORAI1 channels has a major role in the detrimental Ca^{2+} influx caused by oxidative stress. We found that glutamate-resistant HT22R cells exhibit a reduction in SOCE and reduced amounts of ORAI1. Knockdown of ORAI1 protected against two different causes of GSH depletion; blocking cystine uptake with glutamate and inhibiting GSH synthesis with BSO. Pharmacological inhibition of SOCE using the well-established inhibitor 2-APB similarly protected against cell death induced by GSH depletion, but

not against ER stress elicited with the N-glycosylation inhibitor tunicamycin (not shown), which suggests that dysregulation of ORAI1 function is not a general aspect of cell death, despite the fact that glutamate-resistant cells are also resistant against ER stress as well as direct activation of the caspase cascade caused by overexpression of the apoptotic protein BAX.[10] As 2-APB is a known inhibitor of Ca^{2+} influx, its cell survival-promoting action is most probably caused by its inhibitory action on the detrimental Ca^{2+} influx during oxidative stress. This hypothesis is strengthened by our time course experiments, which still showed a beneficial effect of 2-APB when applied up to 8 h after glutamate addition, further pointing to a mechanism of action that interferes with late events in the cell death program such as Ca^{2+} influx. In addition, pCPT-cGMP-induced cell death was prevented by 2-APB, and the observed effect was even stronger than that of the general Ca^{2+} channel blocker $CoCl_2$. Cytosolic elevation of cGMP through increased activity of soluble guanylate cyclases occurs very late in the cell death program induced by glutamate and is responsible for the opening of plasma membrane Ca^2 channels allowing detrimental Ca^{2+} influx.[7]

The fact that knockdown of the upstream initiator of SOCE STIM1 had no effect, speaks against a dysregulation of the whole SOCE machinery and points instead to ORAI1 as the major culprit in these cells. When we investigated the effects of STIM1 and ORAI1 knockdown using the same siRNAs in
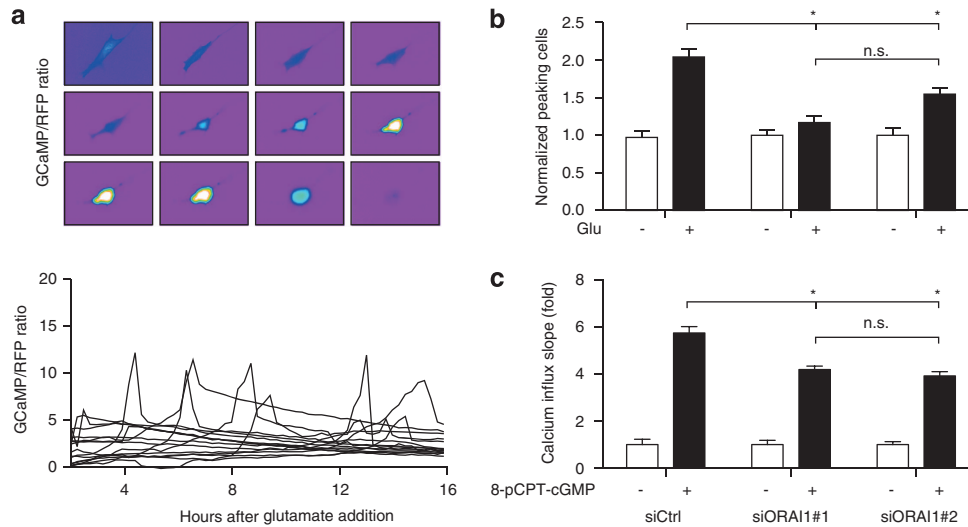
Figure 7 Knockdown of ORAI1 inhibits cytosolic calcium elevation during oxytosis. HT22S cells were transfected with two different siRNAs against ORAI1 or non-targeting siRNA as control together with a plasmid encoding the GCaMP5-IRES-RFP Ca^{2+} reporter gene and subjected to long-term live-cell imaging experiments to show the detrimental Ca^{2+} influx in the late phase of oxidative glutamate toxicity. **(a)** Typical GCaMP pictures of a control siRNA transfected cell under glutamate exposure. The cytosolic Ca^{2+} concentration stays low for several hours, but eventually rises quickly, leading to cell lysis assessed by quenching of the fluorescence signal. The lower panel shows sample traces from glutamate-treated cells transfected with control siRNA, which illustrate the asynchronous appearance of Ca^{2+}-spikes. For reasons of clarity, only Ca^{2+}-peak positive cells from one well are shown. **(b)** Analysis of long-term live-cell imaging of GCaMP-IRES-RFP and siRNA-transfected cells under glutamate exposure in comparison to vehicle treatment. For each picture, a GCaMP5/RFP ratio was calculated. To identify peaking cells, the maximal GCaMP/RFP ratio was divided by the average GCaMP/RFP ratio calculated over the whole measurement period. Each cell that reached a value above the average value of control siRNA transfected cells was counted as Ca^{2+}-peak positive. The amount of Ca^{2+}-peaking cells was normalized to vehicle control and plotted as a bar graph. The bars represent mean ± S.E.M. of 15 replicate wells measured in three independent experiments. **(c)** Analysis of the increase in the GCaMP/RFP ratio in pCPT-cGMP treated HT22 cells transfected with ORAI1 or control siRNA. The slope was normalized to vehicle and plotted as mean ± S.E.M. in bar graphs. Two independent experiments were performed containing >150 cells for each condition. N.S., not significant, *$P < 0.05$ by ANOVA with Tukey's *post hoc* test

mouse embryonic fibroblasts, we observed a detrimental effect for both transcripts, which suggests cell type-specific differences.[23] The protection conferred by ORAI1 knockdown in HT22 cells is in line with the recent observation that CD4-positive T cells from mice lacking ORAI1 robustly proliferate despite repetitive stimulations, and are strongly resistant against stimulation-induced cell death.[24] Our results suggest that ORAI1-mediated Ca^{2+} influx causes cytotoxic Ca^{2+} overload late in the course of oxidative stress-induced cell death. To prove this hypothesis, we performed long-term live-cell imaging of glutamate challenged cells transfected with a genetically-encoded cytosolic Ca^{2+} sensor. The direct observation of cytosolic calcium dynamics revealed a strong but short-lived calcium rise directly preceding cell death, which appeared completely asynchronously in the cell population within a time frame of $5 - 16\,h$ after the addition of glutamate. This perfectly resembles the time course of 2-APB protection. When applied 8 h after glutamate (Figure 4b), 50% of the cells were still rescued, which can be explained by the apparently random distribution of the final Ca^{2+} rise. Cells that have already opened their gates for external Ca^{2+} are irrecoverable, but those that have not induced Ca^{2+} influx at the time of 2-APB addition can still survive by the blockage of Ca^{2+} channels.

Our quantification of Ca^{2+} dynamics cells during glutamate or pCPT-cGMP treatment revealed a direct impact of ORAI1 expression levels on the Ca^{2+} influx after induction of the cell death program, which is perfectly in line with the protective effect of ORAI1 knockdown in the survival assays. Direct Ca^{2+} imaging over the whole-time course of oxidative

glutamate toxicity also disclosed the time lag between cytosolic Ca^{2+} elevation and cell death. We demonstrated that the cytosolic Ca^{2+} rise directly precedes cell death, visible by disintegration of the plasma membrane and strong fluorescence quenching due to loss of GCaMP5. This short time period between the cytosolic Ca^{2+} signal and cell death suggests a direct detrimental role and renders further signaling events unlikely.

Although we showed that intracellular cGMP contributes to Ca^{2+} channel opening, it remains unclear whether it directly causes the opening of ORAI1 channels in endogenous oxidative stress or whether additional factors are needed. It is possible that the reduced amounts of STIM1 in siRNA-transfected cells (Figure 6a, b) are still sufficient to open ORAI1 channels during oxidative stress or that STIM2 can substitute for STIM1 under these conditions. Furthermore, ORAI1 might not only be activated by STIM1, but also through other factors such as the Ca^{2+}-independent phospholipase A_2 (iPLA2β).[25] Also a direct influence of the cellular redox state on ORAI1 activity seems possible. One study revealed that H_2O_2 enhanced I_{CRAC}-mediated Ca^{2+} influx (the electrophysiological equivalent of SOCE) through activation of IP3 receptors and subsequent store depletion without direct effect on ORAI1.[26] SERCA pumps in contrast were shown to be inhibited by H_2O_2.[27] One might speculate that during glutamate-induced oxidative stress, SERCA is inhibited and IP3 receptors activated, which eventually results in ER Ca^{2+} store depletion triggering ORAI1-mediated detrimental Ca^{2+} influx. This would be in line with our results, where 8 h of glutamate treatment resulted in a reduction of the

8

thapsigargin-releasable Ca^{2+} pool, implying reduced SERCA activity or increased ER Ca^{2+} efflux. Others, however, suggested a direct inhibitory effect of H_2O_2 on ORAI1-mediated Ca^{2+} influx induced by store depletion with thapsigargin, which was explained by the oxidation of cysteine residues located in an extracellular loop of ORAI1.[28] This could be interpreted as an attempt to withstand the cytotoxic Ca^{2+}-mediated by ORAI1.

We conclude from the presented data that dysregulated ORAI1-mediated Ca^{2+} influx contributes in a significant manner to programmed cell death induced by GSH depletion in neuronal cells. As this detrimental Ca^{2+} influx occurs late in the course of the cell death program, it might be amenable to therapeutic intervention in acute diseases where oxidative stress have a role.

Materials and Methods

Cell culture. The glutamate-resistant HT22R cell line was generated from the parental mouse hippocampal cell line HT22 as previously described.[19] Both cells lines, HT22S and HT22R, were cultured in DMEM high glucose (PAA Laboratories, Pasching, Austria) supplemented with 5% fetal calf serum (Thermo Fisher Scientific, Waltham, MA, USA) and 100 U per ml penicillin and 100 μg per ml streptomycin (Gibco, Darmstadt, Germany) in a humidified incubator with 5% CO_2 and 95% air.

Cell survival assays. HT22 cells were seeded in 96-well plates at a density of 5000 cells/well and 24 h later subjected to cell death experiments. siRNA-transfected cells were seeded 24 h post transfection. Pharmacological agents were added together with, or at indicated time periods after, induction of cell death by the indicated drugs. Cell viability was quantified 16–24 h after stress onset with the cell titer blue (CTB) reagent (Promega, Madison, WI, USA). Alternatively, in some experiments, the 3-(4,5-Dimethylthiazol-2-yl)-2,5-diphenyltetrazolium bromide (MTT) assay was used.[19] For CTB fluorescence, emission was measured at 590 nm after excitation at 562 nm using a GENios Pro microplate reader (Tecan, Männedorf, Switzerland); for the MTT-assay, absorption was measured at 570 nm.

Calcium live-cell imaging. Fura2 Ca^{2+} imaging experiments were performed on a BD Pathway 855 High Content Imaging System (BD Biosciences, Heidelberg, Germany). The cells were seeded in 96-well imaging plate (BD Bioscience) the day before the experiment in a density of 5000 cells/well and loaded with 5 μM Fura2-AM (Molecular Probes, Darmstadt, Germany) in HBSS for 30 min before the experiment. Measurement was performed with excitation at 340 and 380 nm for ratiometric analysis and pictures were taken with a delay of 5 s. For comparison of SOCE in HT22S and HT22R, cells were seeded on 12 mm coverslips at a density of 100 000/well, loaded with Fura2-AM and placed into a flow chamber. The measurement was performed using an Olympus IX81 fluorescence microscope with the cell^R imaging software. Images were acquired at 340 and 380 nm excitation and the ratio was calculated every 5 s for every single cell. After 1 min of baseline recording, ER-calcium stores were depleted in EGTA buffer (Ca^{2+}-free HBSS supplemented with 0.5 mM EGTA, 20 mM HEPES, 1 mM $MgCl_2$ and 1 g per l Glucose) with 2 μM thapsigargin for 6 min and subsequently Ca^{2+} was readded by changing the buffer to HBSS.

Electrophysiology. We used whole-cell patch clamping to measure currents through ion channels of single cells. Whole-cell recordings were performed using an Axopatch 200B patch clamp amplifier (Axon Instruments, Sunnyvale, CA, USA) and digitized with Digidata 1332 (Axon Instruments). For SOC channels recordings the pipette solution contained (in mM) 120 CsCl, 5 Bapta-Na, 30 Cs-HEPES pH 7.3, 1.5 $MgCl_2$, 4 Na_2ATP, 0.4 Na_2GTP and 1.6 $CaCl_2$ (pCa 7.0). Extracellular solution contained (in mM) 140 NMDG-Asp, 10 $BaCl_2$, 10 Cs-HEPES, pH 7.3. During recording the currents were sampled at 5 kHz and filtered digitally at 500 Hz, the pClamp9 software (Axon Instruments) was used for data acquisition and analysis. In all whole-cell experiments the holding potential was -40 mV, periodically (once every 5 s) the membrane potential was stepped to -100 mV (for 30 ms) and a 200 ms voltage ramp to $+100$ mV was applied. Currents were evoked by application of 1 μM thapsigargin (Sigma, Munich, Germany) in external

solution, which was added to the bath perfusion. The traces recorded before current activation were used as templates for leak subtraction. Whole-cell currents were normalized to the cell capacitance. The mean value of cell capacitance was 19 pF ± 5 (total number of experiments $n = 20$).

Quantitative RT-PCR. Whole-cellular RNA was isolated using ZR RNA MiniPrep Kit (Zymo, Irvine, CA, USA) and transcribed into cDNA with the High Capacity cDNA Reverse Transcription Kit (Applied Biosystems, Darmstadt, Germany). RT-PCR analysis was performed on a 7500 Fast cycler (Applied Biosystems) with FAST BLUE qPCR MasterMix (Eurogentec, Cologne, Germany) running the 7500 standard program. Primers and Probes for STIM1 and 2, ORAI1 and TRPM7 were designed by the universal probe library assay design center (Roche, Mannheim, Germany) and the hypoxanthine-phosphoribosyltransferase gene (HPRT) served as an endogenous control with individually designed primers and probe purchased from MWG (Ebersberg, Germany).

siRNA transfections. Flexitube siRNAs against ORAI1, STIM1, STIM2 and TRPM7 were purchased from Qiagen (Hilden, Germany) (no.SI00972251, no.SI00972272, no.SI1435623, no.SI1435637, no.SI01435665, no.SI01435672, no.SI02694727 and no.SI02742663) and transfected into cells with Lipofectamine RNAiMAX (Invitrogen, Darmstadt, Germany) when cells were grown to 70–80% confluence in six-well plates. Successful knockdown was verified by RT-PCR or immunoblot.

Immunoblotting. Cells were lysed in ice-cold RIPA buffer (Thermo Fisher Scientific) containing mini complete protease inhibitor cocktail (Roche) and centrifuged for 30 min at 16 000 g. The supernatants were separated on 8–16% polyacrylamide gels (Thermo Fisher Scientific), transferred onto nitrocellulose membranes with the iBlot System (Invitrogen, Darmstadt, Germany) and blocked in 3% nonfat dry milk in phosphate-buffered saline containing 0.5% Tween-20 (PBS-T) for 1 h at room temperature before overnight incubation with primary antibodies against STIM1 (BD Biosciences, no.610955 1:250), STIM2 (Cell Signaling, Danvers, MA, USA, no.4917 1:1000), ORAI1, Alomone Jerusalem, Israel, no.ACC-062 1:500), Actin (Millipore, Billerica, MA, USA, no.MAB1501 1:5000) or GAPDH (Cell Signaling, no.2118 1:5000) followed by α-mouse (respectively rabbit) IgG (Fc) infrared fluorescence − conjugated secondary antibody (Licor, Lincoln, NE, USA, 1:30 000). The membranes were scanned for infrared fluorescence at 680 or 800 nm using the Odyssey system (Licor) and the signal was analyzed quantitatively with the image-processing software ImageJ (http://rsbweb.nih.gov/ij/).

Long-term calcium live-cell imaging. GCaMP5 was a kind gift of Douglas S. Kim (Howard Hughes Medical Institute, Ashburn) and subcloned with EcoRI and NotI into the IRES-RFP-containing vector PB531A-1 (System Biosciences, Mountain View, CA, USA). Cells were transfected with GCaMP5-IRES-RFP together with two different siRNAs against ORAI1 or non-targeting control-siRNA with Lipofectamine 2000 (Invitrogen) in six-well plates and 24 h later transferred to 96-well imaging plates (BD Biosciences) at a density of 5000 cells/well. For calcium imaging, phenol red containing medium was replaced by colorless DMEM (PAA Laboratories, Pasching, Austria). Two hours before the onset of measurement, 25 mM glutamate was added to the cells, control wells were supplemented with vehicle and the plate was incubated in the BD Pathway 855 at 37 °C with 5% CO2 and 95% air. For pCPT-cGMP-induced Ca^{2+} influx, measurement was started immediately after addition of 2.5 mM pCPT-cGMP. Cytosolic calcium was monitored by GCaMP5 and normalized to RFP fluorescence; pictures were taken every 15 min. For analysis of glutamate-induced Ca^{2+} peaks, the maximal ratio was divided by the average ratio and a threshold was defined by the mean of control-siRNA transfected cells. Every cell above that threshold was counted as Ca^{2+} peak positive. For analysis of pCPT-cGMP-induced Ca^{2+} influx, the slope of Ca^{2+} increase was calculated over the first 2 h of the measurement.

Statistical analysis. Data were analyzed as mean ± S.E.M. and the statistical significance assessed using two-tailed t-tests or analysis of variance (ANOVA) with Tukey's Multiple Comparison Test as indicated.

Conflict of Interest

The authors declare no conflict of interest.

1. Dringen R. Metabolism and functions of glutathione in brain. *Prog Neurobiol* 2000; **62**: 649–671.
2. Dixon SJ, Lemberg KM, Lamprecht MR, Skouta R, Zaitsev EM, Gleason CE et al. Ferroptosis: an iron-dependent form of nonapoptotic cell death. *Cell* 2012; **149**: 1060–1072.
3. Albrecht P, Lewerenz J, Dittmer S, Noack R, Maher P, Methner A et al. Mechanisms of oxidative glutamate toxicity: the glutamate/cystine antiporter system xc- as a neuroprotective drug target. *CNS Neurol Disord Drug Targets* 2010; **9**: 373–382.
4. Tan S, Sagara Y, Liu Y, Maher P, Schubert D. The regulation of reactive oxygen species production during programmed cell death. *J Cell Biol* 1998; **141**: 1423–1432.
5. Li Y, Maher P, Schubert D. A role for 12-lipoxygenase in nerve cell death caused by glutathione depletion. *Neuron* 1997; **19**: 453–463.
6. Pallast S, Arai K, Wang X, Lo EH, van Leyen K. 12/15-Lipoxygenase targets neuronal mitochondria under oxidative stress. *J Neurochem* 2009; **111**: 882–889.
7. Li Y, Maher P, Schubert D. Requirement for cGMP in nerve cell death caused by glutathione depletion. *J Cell Biol* 1997; **139**: 1317–1324.
8. Davis JB, Maher P. Protein kinase C activation inhibits glutamate-induced cytotoxicity in a neuronal cell line. *Brain Res* 1994; **652**: 169–173.
9. Murphy TH, Miyamoto M, Sastre A, Schnaar RL, Coyle JT. Glutamate toxicity in a neuronal cell line involves inhibition of cystine transport leading to oxidative stress. *Neuron* 1989; **2**: 1547–1558.
10. Dittmer S, Sahin M, Pantlen A, Saxena A, Toutzaris D, Pina AL et al. The constitutively active orphan G-protein-coupled receptor GPR39 protects from cell death by increasing secretion of pigment epithelium-derived growth factor. *J Biol Chem* 2008; **283**: 7074–7081.
11. Noack R, Frede S, Albrecht P, Henke N, Pfeiffer A, Knoll K et al. Charcot-Marie-Tooth disease CMT4A: GDAP1 increases cellular glutathione and the mitochondrial membrane potential. *Hum Mol Genet* 2012; **21**: 150–162.
12. Sahin M, Saxena A, Joost P, Lewerenz J, Methner A. Induction of Bcl-2 by functional regulation of G-protein coupled receptors protects from oxidative glutamate toxicity by increasing glutathione. *Free Radic Res* 2006; **40**: 1113–1123.
13. Toutzaris D, Lewerenz J, Albrecht P, Jensen LT, Letz J, Geerts A et al. A novel giant peroxisomal superoxide dismutase motif-containing protein. *Free Radic Biol Med* 2010; **48**: 811–820.
14. Roos J, DiGregorio PJ, Yeromin AV, Ohlsen K, Lioudyno M, Zhang S et al. STIM1, an essential and conserved component of store-operated Ca2 + channel function. *J Cell Biol* 2005; **169**: 435–445.
15. Liou J, Kim ML, Heo WD, Jones JT, Myers JW, Ferrell JE Jr et al. STIM is a Ca2 + sensor essential for Ca2 + -store-depletion-triggered Ca2 + influx. *Curr Biol* 2005; **15**: 1235–1241.
16. Zhang SL, Yeromin AV, Zhang XH, Yu Y, Safrina O, Penna A et al. Genome-wide RNAi screen of Ca(2 +) influx identifies genes that regulate Ca(2 +) release-activated Ca(2 +) channel activity. *Proc Natl Acad Sci USA* 2006; **103**: 9357–9362.
17. Prakriya M, Feske S, Gwack Y, Srikanth S, Rao A, Hogan PG et al. Orai1 is an essential pore subunit of the CRAC channel. *Nature* 2006; **443**: 230–233.
18. Mignen O, Thompson JL, Shuttleworth TJ. Orai1 subunit stoichiometry of the mammalian CRAC channel pore. *J Physiol (Lond)* 2008; **586**: 419–425.
19. Lewerenz J, Klein M, Methner A. Cooperative action of glutamate transporters and cystine/glutamate antiporter system Xc- protects from oxidative glutamate toxicity. *J Neurochem* 2006; **98**: 916–925.
20. Li M, Jiang J, Yue L. Functional characterization of homo- and heteromeric channel kinases TRPM6 and TRPM7. *J Gen Physiol* 2006; **127**: 525–537.
21. Fukushima M, Tomita T, Janoshazi A, Putney JW. Alternative translation initiation gives rise to two isoforms of orai1 with distinct plasma membrane mobilities. *J Cell Sci* 2012; **125**: 4354–4361.
22. Penna A, Demuro A, Yeromin AV, Zhang SL, Safrina O, Parker I et al. The CRAC channel consists of a tetramer formed by Stim-induced dimerization of Orai dimers. *Nature* 2008; **456**: 116–120.
23. Henke N, Albrecht P, Pfeiffer A, Toutzaris D, Zanger K, Methner A et al. Stromal interaction molecule 1 (STIM1) is involved in the regulation of mitochondrial shape and bioenergetics and plays a role in oxidative stress. *J Biol Chem* 2012; **287**: 42042–42052.
24. Kim KD, Srikanth S, Yee MK, Mock DC, Lawson GW, Gwack Y et al. ORAI1 deficiency impairs activated t cell death and enhances T cell survival. *J Immunol* 2011; **187**: 3620–3630.
25. Bolotina VM. Orai, STIM1 and iPLA2beta: a view from a different perspective. *J Physiol (Lond)* 2008; **586**: 3035–3042.
26. Grupe M, Myers G, Penner R, Fleig A. Activation of store-operated ICRAC by hydrogen peroxide. *Cell Calcium* 2010; **48**: 1–9.
27. Kuster GM, Lancel S, Zhang J, Communal C, Trucillo MP, Lim CC et al. Redox-mediated reciprocal regulation of SERCA and Na + -Ca2 + exchanger contributes to sarcoplasmic reticulum Ca2 + depletion in cardiac myocytes. *Free Radic Biol Med* 2010; **48**: 1182–1187.
28. Bogeski I, Kummerow C, Al-Ansary D, Schwarz EC, Koehler R, Kozai D et al. Differential redox regulation of orai ion channels: a mechanism to tune cellular calcium signaling. *Sci Signal* 2010; **3**: ra24.